Proceedings of the ASME 2022 41st International Conference on Ocean, Offshore and Arctic Engineering
OMAE2022
June 5-10, 2022, Hamburg, Germany

OMAE2022-79450

NUMERICAL INVESTIGATION ON SCALE EFFECT OF 5415M MANEUVERABILITY

Donglei Zhang, Qing Wang*, Kai Dong, Xianzhou Wang
School of Naval Architecture and Ocean Engineering
Huazhong University of Science and Technology
Key Laboratory of Ship and Ocean Hydrodynamics of Hubei Province
Wuhan, Hubei, 430074, P. R. of China

ABSTRACT

A numerical investigation about the effect of ship model scale on turning maneuver has been presented in this study. A preliminary US Navy surface combatant, David Taylor Model Basin (DTMB) 5415M, is chosen as the object of study. An in-house computational fluid dynamics (CFD) solver is used for the numerical simulation. Structured grid has been divided for the model and the use of overset grid technology allows the deflection of the rudders when the surface combatant undergoes 6 degrees of freedom motions. Numerical modelling errors for the simulation of steady turning at 35-degree deflection of DTMB 5415M rudder at Fr=0.41 in calm water have been estimated. The grid convergence studies have been conducted for the uncertainty analysis and the numerical results have been compared with the existed experimental data, which showed a good agreement. Three different scales (1:5, 1:15, 1:35.48) have been selected for the investigation to study the scale effects on ship turning maneuvers. Ship motions, hydrodynamic forces and moments for all the scales have been compared for the purpose of analyzing the scale effects on ship maneuverability. The results show that larger scale has smaller tactical diameter and smaller roll angle. The results of intermediate scale are less than 5% compared with the smallest scale, and the difference between the largest scale and the smallest scale is more than 10%, especially the roll angle reaches 50%. The scales have different influence on forces coefficient and moment coefficient of different directions.

Keywords: CFD; DTMB 5415M; Turning; Scale effect; Overset grid.

NOMENCLATURE

x, y, z	Direction of cartesian coordinate systems
u, v, w	Linear velocity in x, y, z direction
$\dot{u}$, $\dot{v}$, $\dot{w}$	Linear acceleration in x, y, z direction
p, q, r	Angular velocity in x, y, z direction
$\dot{p}$, $\dot{q}$, $\dot{r}$	Angular acceleration in x, y, z direction
t	Physics time(s)
r*	$r \times L_{PP}/u_0$, steady yaw rate
t*	$t \times u_0/L_{PP}$
x^*, y^*	x/L_{pp}, y/L_{pp}
ρ	Density of water
g	Gravity acceleration
ν	Kinematic viscosity
P	Pressure
S	Pressure
Cp	$\frac{P}{0.5\rho v^2 S}$, pressure coefficient
I_x, I_y, I_z	Ship moment of inertia about x-, y-, z-axis
K_T, K_Q	Torque coefficient, thrust coefficient
L_{PP}	Length between perpendiculars(m)
u_0	Ship service speed(m/s)
Fr	$\frac{u_0}{\sqrt{gL_{PP}}}$, Froude number
Re	$\frac{u_0 L_{PP}}{\nu}$, Reynolds number
X, Y, Z	Forces acting on the hull in x, y, z direction
X^*, Y^*, Z^*	$\frac{X}{0.5\rho v^2 S}$, $\frac{Y}{0.5\rho v^2 S}$, $\frac{Z}{0.5\rho v^2 S}$, force coefficient
K, M, N	Moments acting on the hull in x, y, z direction
K^*, M^*, N^*	$\frac{K}{0.5\rho v^2 L_{pp} S}$, $\frac{M}{0.5\rho v^2 L_{pp} S}$, $\frac{N}{0.5\rho v^2 L_{pp} S}$, moment coefficient

1. INTRODUCTION

Predicting ship maneuverability is one of the important topics in ship engineering. However, because of the difference between model and full scale Reynolds number (Re), phenomena concerning viscosity cannot be similar. So, it is

* Contact author: qingwang@hust.edu.cn

difficult to predict full scale ship maneuverability using conventional methods such as model test. Many researchers had struggled and tried to reveal the scale effect on ship maneuverability for many years

Hoppe, K.G. [1] outlines a method to compensate for scale effects caused by viscosities with particular emphasis on maneuvering tests. Kajita, E. et al. [2] investigated the scale effect on the normal force of rudder and the flow around rudder had been analyzed from the records of rudder force generated by a steering.

Jin, Y. et al. [3] investigates the influence of ship model size on maneuvering hydrodynamic coefficients utilizing a Reynolds Averaged Navier–Stokes solver. The hydrodynamic forces and yaw moment on KVLCC2 model have been predicted for a static drift and a pure sway test and validated against benchmark model scale test data. A set of systematic simulations on different size KVLCC2 ship models and the full scale vessel has been carried out for pure sway, static drift and pure yaw tests to study the scale effects on the hydrodynamic forces and moments obtained from the captive maneuvers.

Liu, X. et al. [4] conducted the comparing research on ship maneuvering between full scale ship and the model for the YUKUN training ship. Based on the data of both sea trial and model test, the trajectory, roll, pitch, RPM and the power of the main engine were compared. Some difference between full scale and model ship was found, and linear method was adopted to make a correction for model test.

Duman, S. et al. [5] investigated the effects of ship-model scale ratios on hydrodynamic maneuvering coefficients numerically. Unsteady Reynolds-Averaged Navier-Stokes (URANS) approach had been employed in order to calculate the hydrodynamic forces and moments acting on the well-known naval surface combatant DTMB 5415 hull. Static drift tests had been simulated for a different model scale. The forces and moments obtained from the numerical analyses had been used to calculate the maneuvering coefficients. The influences of ship-model ratio had been discussed. In addition, wave deformations along the hulls at different static drift conditions have been investigated.

Araki, M. [6] conducted captive maneuvering simulations in different scales KVLCC2 by applying RANS solver NAGISA with the overset gird method. The maneuvering coefficients and flow field predicted in different scales are compared in detail to analyze the scale effect on ship maneuverability.

Generally, previous studies focus on difference of hydrodynamic maneuvering forces and moments coefficients between different scales though captive maneuvers simulation. In this study, our work investigates the scale effects on turning maneuver of DTMB 5415M by using an in-house CFD solver, which using second order finite difference method to discrete the continuous medium, using projection algorithm to solve the pressure-velocity coupling equation, and using level-set method to capture the free surface. Many previous articles have demonstrated the accuracy and ability of the solver, more details are described in Ref. (7-9). The grid convergence studies have been conducted for the uncertainty analysis. The simulation results have been compared with the existed experimental fluid dynamics (EFD) date, which showed a good agreement. Three different scales (1:5, 1:15, 1:35.48) have been selected for the computation. Ship motions, hydrodynamic forces and moments for all the scales have been predicted to analyze the influence of different Reynolds number.

2. COMPUTATIONAL METHOD

2.1 Governing Equations

RANS equations are applied in this study and the continuity equation for mean velocity of the unsteady, three-dimensional incompressible flow. The continuity equation and momentum equations in Cartesian coordinates can be given as:

$$\frac{\partial \rho}{\partial t}+\frac{\partial(\rho U_i)}{\partial x_i}=0 \tag{1}$$

$$\frac{\partial U_i}{\partial t}+\frac{\partial U_i U_j}{\partial x_j}=-\frac{1}{\rho}\frac{\partial P}{\partial x_i}+\frac{1}{\rho}\frac{\partial}{\partial x_j}\left(\mu\frac{\partial U_i}{\partial x_j}-\rho\overline{u_i' u_j'}\right) \tag{2}$$

where U_i and u_i' (i =1, 2, 3) are the time-averaged and fluctuation components of velocities, respectively, ρ means the fluid density, P is the time-averaged pressure, μ is the dynamic viscosity, and $\rho\overline{u_i' u_j'}$ is the Reynolds stress term.

In the study, SST *k-ω* two equations turbulent model [10] is used to solve the RANS equations, which can be automatically converted between the k-ε model and the k-ω model by the hybrid function, the predicted boundary layer is turbulent, and the flow separation from the hull can be predicted.

2.2 Ship 6DOF Motion Equations

Two right-handed Cartesian coordinate systems are used to describe the 6DOF motion of the surface combatant, as shown in Figure 2. Ship motion equations are:

$$m[\dot{u}-vr+wq]=X \tag{3}$$

$$m[\dot{v}-wp+ur]=Y \tag{4}$$

$$m[\dot{w}-uq+vp]=Z \tag{5}$$

$$I_x\dot{p}+[I_y-I_z]qr=K \tag{6}$$

$$I_y\dot{q}+[I_x-I_z]rp=M \tag{7}$$

$$I_z\dot{r}+[I_z-I_x]pq=N \tag{8}$$

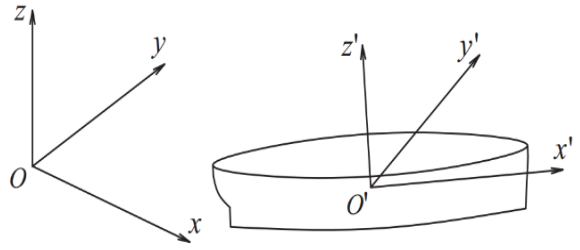

FIGURE 1: THE COORDINATE SYSTEM OF SHIP MOTION

Where $\boldsymbol{m}$ is the total mass of the surface combatant; $\boldsymbol{I_x}$, $\boldsymbol{I_y}$ and $\boldsymbol{I_z}$ are the moment of inertia about x- axis, y- axis and z-axis. $\boldsymbol{X}$, $\boldsymbol{Y}$, $\boldsymbol{Z}$ are the forces and moments acting on the hull in x, y, z direction. $\boldsymbol{K}$, $\boldsymbol{M}$, $\boldsymbol{N}$ are the moments acting on the hull in x, y, z direction respectively.

2.3 Body-force Method

Propellers are modeled through body-force method in which local velocity effects on the propellers are neglected. The open water curves are expressed as polynomials [1], $K_T \; or \; K_Q = a_0 + a_1 J + a_2 J^2 + a_3 J^3 + a_4 J^4 + a_5 J^5$; $J = V/nD$ .The details are provided in Table 1.

TABLE 1: RESULTS OF PROPELLER OPENWATER TEST

	K_T	K_Q
a_0	0.398399	0.051144
a_1	-0.067794	-0.000390
a_2	-1.286040	-0.171650
a_3	2.286960	0.330060
a_4	-2.039820	-0.327865
a_5	0.676134	0.119477

3. GEOMETRY AND CONDITION

3.1 Computational Model

The hull geometry is the fully appended DTMB 5415M [1], which is the European version of DTMB 5415. DTMB 5415 has been used as a benchmark for decade and has a lot of existed EFD data. The DTMB 5415M shares the same hull, but the appendages and propellers are redesigned. Three different scales have been selected for the investigation to study the scale effects on ship maneuvers. Table 2 presents the relevant information in the different scales and the profile of the ship model is shown in Figure 2.

TABLE 2: DTMB 5415M PRINCIPAL DIMENSIONS IN DIFFERENT SCALES

	Model 1	Model 2	Model 3
λ	5	15	35.48
L_{pp}(m)	28.40	9.467	4.002
B_{wl}(m)	3.812	1.271	0.537
T(m)	1.230	0.410	0.173
D(m^3)	1684.9	561.6	0.189
S_w(m^2)	594.5	198.2	2.361
GM(m)	0.390	0.130	0.055
LCG(m)	-0.130	-0.043	-0.018

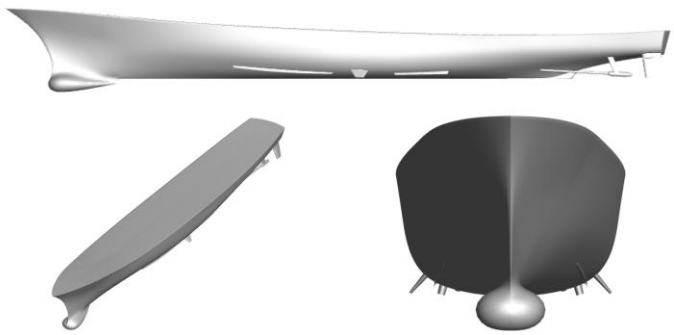

FIGURE 2: GEOMETRY OF DTMB 5415M

3.2 Grid and Condition

Overset mesh technique has been used in this study, which allows complex motions when the ship under 6DOF. Structured grid has been generated separately for the model hull, appendage and numerical tank. Due to its simple logic and strong adaptability, structured mesh can provide more accuracy for simulation results.

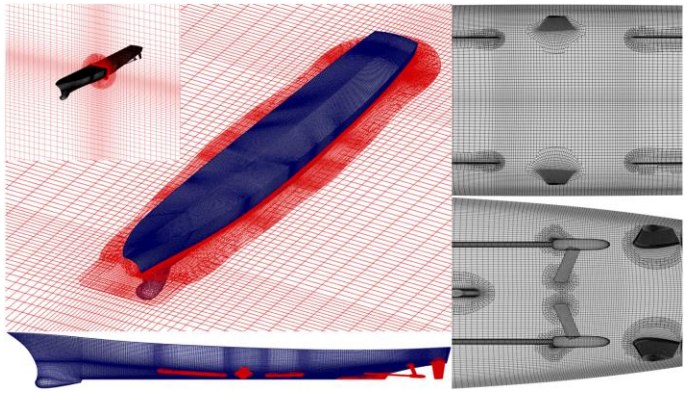

FIGURE 3: OVERSET MESH AND SURFACE GRID OF DTMB 5415M

The structural overset mesh and surface grid of DTMB 5415M are given in Figure 3. The grids around the ship hull and the computational grid are generated separately, and with the overset program, the two different grids are united. The fixed no-slip is imposed on the hull surface of DTMB 5415M. The velocity inlet is imposed in front of the numerical tank. The pressure outlet is imposed on the tail of numerical tank. The zero-pressure is imposed on the bottom of the numerical tank, while the zero-pressure gradient is imposed on the top and sides of the numerical tank. Figure 4 shows the boundary conditions of the numerical tank in detail.

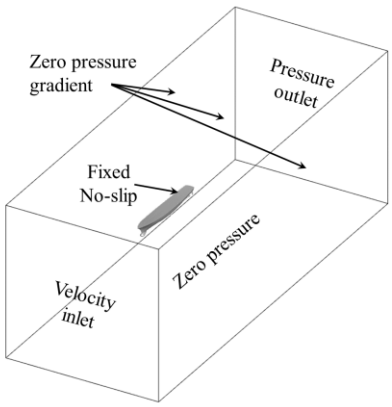

FIGURE 4: BOUNDARY CONDITION OF NUMERICAL TANK

The computation domain extends for $1.0L_{pp}$ in the front of the ship hull, $3.0L_{pp}$ behind the hull, $1.0L_{pp}$ to the side and $1.15L_{pp}$ under the keel of the model. The air layer extends $0.65L_{pp}$ above the calm water surface. In order to investigate the scale effect of ship maneuverability, three different scales have been selected. Turning at 35-degree rudder deflection at Fr=0.41 in calm water had been conducted. Table 3 shows the

computational conditions, the y+ values and the number of grids when modeling the model at different scales, and the dimensionless first layer grid heights $\overline{\Delta y_1}$ are calculated by:

$$\overline{\Delta y_1} = y^+ \times 8.721 \times Re^{-0.9286} \quad (9)$$

In the calculation process, the computer resource used for one case is about 48 cores for two weeks.

TABLE 3: SIMULATION CONDITIONS OF THREE DIFFERENT SCALES

	λ=5	λ=15	λ=35.48
L_{pp}(m)	28.40	9.47	4.00
u_0(m/s)	6.90	3.98	2.59
Fr	0.41	0.41	0.41
Re	1.96×10^8	3.74×10^7	1.04×10^7
Wall Function	Yes	No	No
y^+	40	1	1
Grid Amounts	9.8M	9.0M	6.6M

4. VERIFICATION AND VALIDATION STUDY

Three different structured grids were applied to predict the ship maneuverability in the verification study to verify the accuracy of the in-house CFD solver. Three different grids are used to simulate the turning maneuver based on the smallest model scale (1:35.48) in the same turbulence model and same time step. Test condition is turning at 35-degree rudder deflection at Fr=0.41 in calm water, which is the same in following work. Figure 5, 6 and 7 show the trajectories, roll angle and yaw rate in three different grids respectively.

In this study, the grid space uncertainty will be obtained by analyzing tactical diameter, steady roll angle and steady yaw rate. Systematic grid-spacing study was carried out applying the Richardson extrapolation method [11].

4.1 Numerical Uncertainty

At the start, the uniform parameter refinement ratio r_k between results predicted by different grids is assumed:

$$r_k = \frac{\Delta x_2}{\Delta x_1} = \frac{\Delta x_3}{\Delta x_2} \quad (10)$$

Where Δx_1 is the coarse grid spacing, Δx_2 is the medium grid spacing and Δx_3 is the fine grid spacing. S_1, S_2 and S_3 are the solutions predicted by coarse mesh, medium mesh and fine mesh spacing. $\varepsilon_{21} = S_2 - S_1$ and $\varepsilon_{32} = S_3 - S_2$ are differences between medium-fine and coarse-medium results. R is convergence ratio whose definition is expressed as the following formula:

$$R = \frac{\varepsilon_{32}}{\varepsilon_{21}} \quad (11)$$

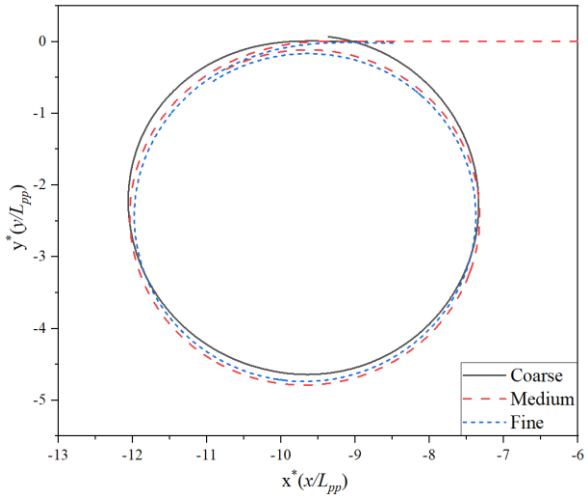

FIGURE 5: PREDICTED TRAJECTORIES FOR TURN MANEUVER IN DIFFERENT GRIDS

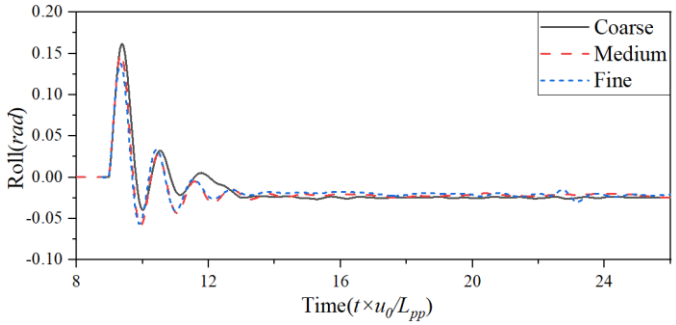

FIGURE 6: TIME DOMAIN CURVE OF ROLL ANGLE PREDICTED BY DIFFERENT GRIDS

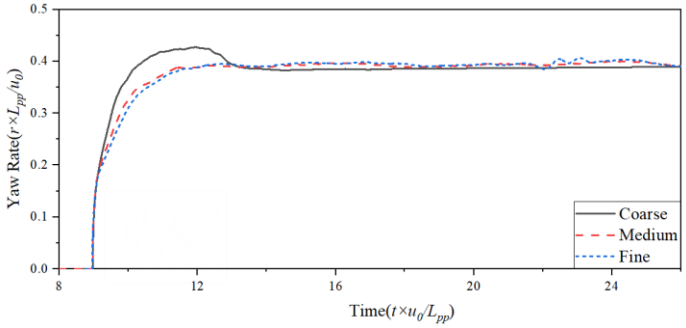

FIGURE 7: TIME DOMAIN CURVE OF YAW RATE PREDICTED BY DIFFERENT GRIDS

There are three possible convergence conditions:
Monotonic convergence (MC): $0 < R < 1$
Oscillatory convergence (OC): $R < 0$
Divergence (D): $1 < R$

When 0<R<1, monotonic convergence is achieved and Richardson extrapolation method can be used. P_{RE} is used to indicate the estimated order of accuracy which is given as:

$$P_{RE} = \frac{\ln(\varepsilon_{21}/\varepsilon_{32})}{ln\ r_k} \quad (12)$$

The ratio of P_{RE} to P_{th} is used to indicate the distance metric P:

$$P = \frac{P_{RE}}{P_{th}} \tag{13}$$

Where P_{th} is an estimation of the limiting order of accuracy when spacing size goes to zero. Usually, P_{th} equals to two. The factor of safety method uncertainty is calculated as:

$$U_{FS} = \begin{cases} (2.45 - 0.85P)\left|\dfrac{S_f - S_E}{r^{P_{RE}} - 1}\right|, & 0 < P \le 1 \\ (16.4P - 14.8)\left|\dfrac{S_f - S_E}{r^{P_{RE}} - 1}\right|, & P > 1 \end{cases} \tag{14}$$

The experimental results S_E from Carrica, P.M. [12] are chosen to analyze the magnitude of uncertainty. Three sets of structured grids were applied to the grid uncertainty study of the simulation of turning circle maneuver. In the computation, the growth rate and the number of grid layers are changed in three directions with the grid refinement ratio $\sqrt{2}$ corresponding to coarse. The results predicted by different grids are shown in Table 4.

TABLE 4: RESULTS PREDICTED BY DIFFERENT GRIDS

		Tactical diameter (L_{pp})	Steady roll angle (rad)	Steady yaw rate r^* ($r \times L_{pp}/u_0$)
Coarse grid	S_1	4.860	-0.0234	0.385
Medium grid	S_2	4.716	-0.0206	0.393
Fine grid	S_3	4.665	-0.0195	0.396
R		0.354	0.393	0.375
P		1.498	1.349	1.416
$U_{FS}(S_E\%)$		5.835	2.603	3.788
Convergence conditions		MC	MC	MC

4.2 Validation Study

Next, the results of tactical diameter are selected for validation study. The comparison error E was defined as:

$$E = |S_E - S| / S_E \tag{15}$$

where S is the CFD result, S_E .is the EFD result. To determine whether validation has been completed, E is compared to the validation uncertainty U_V, while the U_V was presented as:

$$U_V^2 = U_D^2 + U_{SN}^2 \tag{16}$$

The uncertainty of experimental data U_D is not presented in the experiment, so U_D is assumed as 1.00% S_E. U_{SN} was defined as estimated numerical uncertainty, U_{SN} here is equal to U_{FS}. The results of validation study are shown in Table 5 and the comparison error E is lower than the validation uncertainty U_V, which shows that the simulation results have been verified under U_V level, which indicates that the results are reliable.

TABLE 5: VALIDATION STUDY RESULTS

U_{SN} (%S_E)	U_D (%S_E)	U_V (%S_E)	E (%S_E)
5.835	1	5.919	0.705

From the results of the Table 4 and considering the consumption of computational resources and time, we can see that the medium grid is the most suitable condition for the follow-up numerical computation.

4.3 Comparation with Experimental Results

The numerical simulation results of medium grid have been compared with the experimental results conducted by Carrica, P.M. et al. [12]. And the accuracy of the CFD method is verified. The predicted trajectories, roll angle and yaw rate are shown in the figure 8, 9 and 10 respectively. Table 6 shows the specific values of CFD and EFD results.

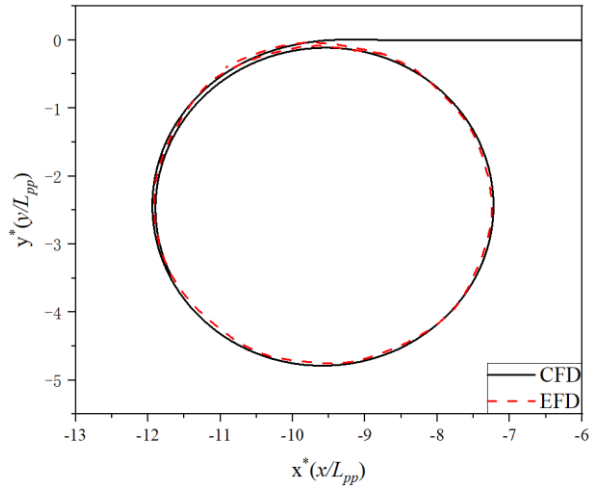

FIGURE 8: PREDICTED TRAJECTORIES VERSUS EFD DATA FOR TURN MANEUVER

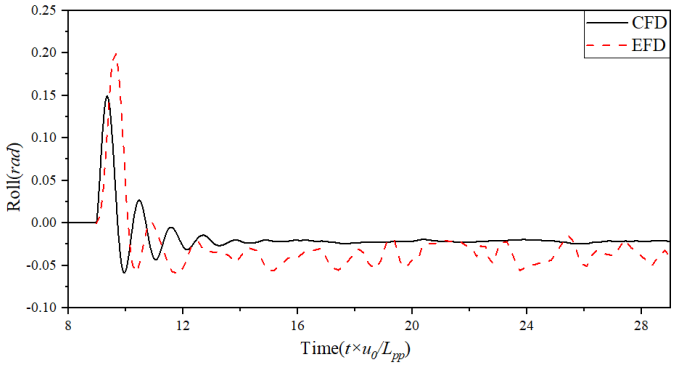

FIGURE 9: TIME DOMAIN CURVE OF THE PREDICTED ROLL ANGLE VERSUS EFD DATA

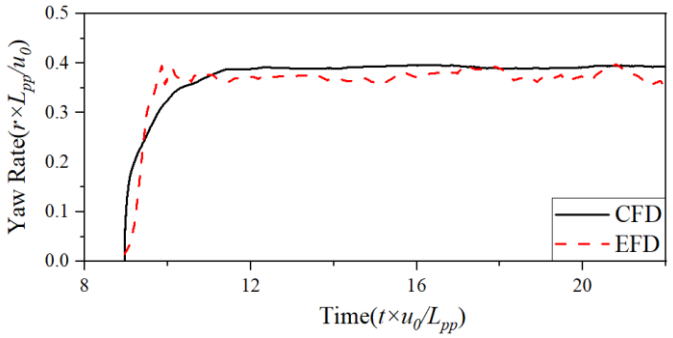

FIGURE 10: TIME DOMAIN CURVE OF THE PREDICTED YAW RATE VERSUS EFD DATA

TABLE 6: CFD RESULTS VERSUS EXPERIMENTAL DATA

	CFD	EFD	error
Tactical diameter (L_{pp})	4.716	4.683	0.71%
Advance (L_{pp})	3.173	3.099	2.39%
Transfer (L_{pp})	2.061	1.993	3.41%
Max yaw rate r^* ($r \times L_{pp}/u_0$)	0.400	0.402	-0.50%

The results show that the simulation results are in good agreement with the exited EFD data. The error of predicted tactical diameter and max yaw rate are around 1%, meanwhile the error of advance and transfer is less than 5% which proves that the CFD method used here is reliable enough.

5. RESULTS AND DISCUSSION

In order to study the scale effects of ship maneuverability, the simulations of turning at 35-degree rudder deflection at Fr=0.41 in calm water were performed for the three scale models (1:5,1:15,1:35.48). The trajectories, roll angle and yaw rate of turning circle maneuver in three different scales are shown in Figure11, 12 and 13 respectively.

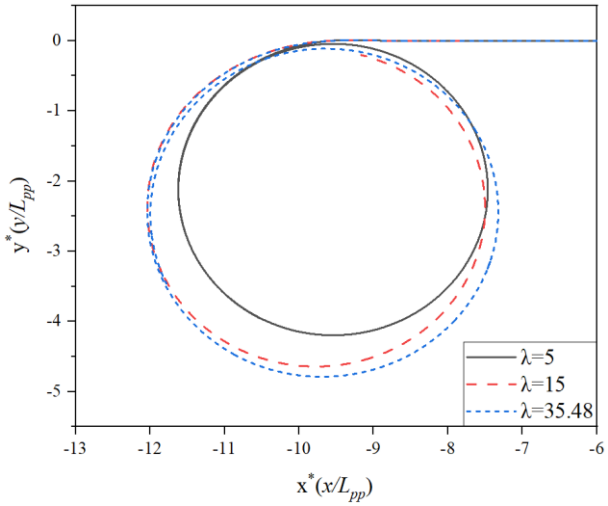

FIGURE 11: PREDICTED TRAJECTORIES FOR TURN MANEUVER IN DIFFERENT SCALES

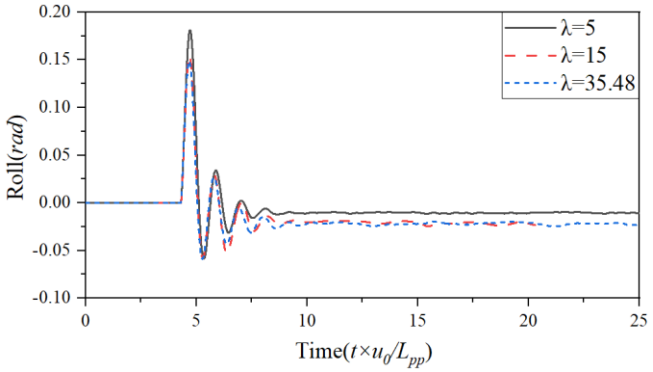

FIGURE 12: TIME DOMAIN CURVE OF THE ROLL ANGLE PREDICTED IN DIFFERENT SCALES

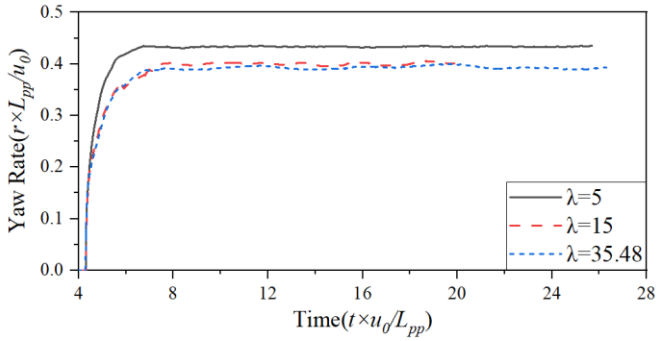

FIGURE 13: TIME DOMAIN CURVE OF THE YAW RATE PREDICTED IN DIFFERENT SCALES

Table 7 show the tactical diameter, steady yaw rate and steady roll angle in three different scales.

TABLE 7: SIMULATION CONDITIONS OF THREE DIFFERENT SCALES

	λ =5	**λ=15**	**λ=35.48**
Tactical diameter (L_{pp})	4.157	4.536	4.716
Steady yaw rate r^* ($r \times L_{pp}/u_0$)	0.4334	0.4023	0.3937
Steady roll angle (rad)	-0.0105	-0.0221	-0.0218

Scale of 1:35.48 has the largest tactical diameter, appearing as a larger scale a smaller diameter. The roll angle for 1:15 and 1:35.48 are very similar, which is larger than 1:5. The yaw rates for 1:15 and 1:35.48 are similar too, which is smaller than 1:5.

The results of intermediate scale are less than 5% compared with the smallest scale, and the difference of predicted results between largest scale and smallest scale is more than 10%, especially the roll angle reaches 50%. This phenomenon occurs because the Reynolds numbers of two small-scale are closer, while difference between Re is the main factor leading to scale effect. The pressure distribution (Cp is the pressure coefficient) on the bottom surface of the hull for the three scale models is shown in Figure 14, it can be seen that the scale effect also has an influence on the pressure distribution.

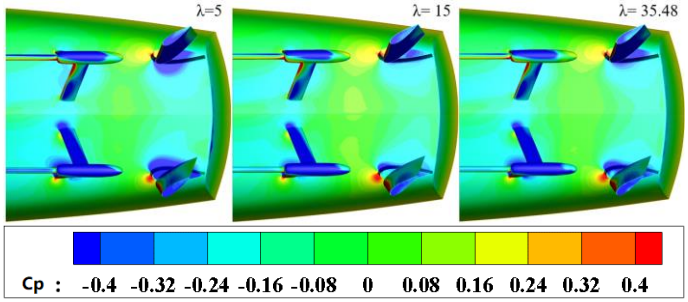

FIGURE 14: SURFACE PRESSURE OF TURNING CIRCLE MANEUVER IN DIFFERENT SCALES

Table 8 shows the sway force coefficient, yaw moment coefficient on hull and surge, sway, heave force coefficient and roll, pitch, yaw moment coefficient on rudder.

TABLE 8: MOMENT COEFFICIENT AND FORCE COEFFICIENT ON HULL AND RUDDER

	Coefficient	λ=5	λ=15	λ=35.48
Hull+ Rudder	$Y^*(\times 10^{-2})$	-1.578	-1.458	-1.408
	$N^*(\times 10^{-5})$	1.784	1.451	1.258
Rudder	$X^*(\times 10^{-1})$	2.416	2.149	1.896
	$Y^*(\times 10^{-1})$	3.626	2.867	2.286
	$Z^*(\times 10^{-2})$	-2.591	-2.176	-1.753
	$K^*(\times 10^{-3})$	12.121	9.648	7.788
	$M^*(\times 10^{-3})$	4.357	3.343	2.185
	$N^*(\times 10^{-1})$	1.786	1.421	1.139

The differences in force and moment coefficient on hull at different scales are smaller than that on the rudder. Because of the much smaller Reynolds number compared to larger scale, the model scale produces a thicker boundary layer. The difference in the frictional resistance coefficient has to be balanced by different propeller load at different scales, which causes differences in the force coefficients and moment coefficients acting on the rudder by the wake at different scales.

The results show that the differences of surge, heave force coefficient between different scales are not so evident, while the differences of sway forces coefficient and roll, pitch, yaw moment coefficient between different scales are significant. The differences in force and moment coefficient lead to the different motions in different scale.

6. CONCLUSION

The main purpose of this study is to analyze the scale effects on ship maneuverability by simulating turn maneuver of different scale DTMB 5415M models. An in-house CFD solver is used to solve the governing equations coupled with ship 6DOF motion equations

Verification and validation study were carried out and the prediction of turn maneuvers show good agreement with the existed EFD results, which means the solver has a good ability to predict ship maneuverability. Three different scales have been selected for the investigation to study the scale effects on ship turning maneuvers. Larger scale has smaller tactical diameter due to larger yaw rate and has smaller roll angle. The results of intermediate scale are less than 5% compared with the smallest scale, and the difference of predicted results between the largest scale and the smallest scale is more than 10%, especially the roll angle reaches 50%. The differences of sway forces coefficient and yaw moment coefficient between different scales are evident.

Future work includes prediction of ship maneuverability in shallow water and wave conditions for the purpose of studying the fluid characteristic effects on the ship maneuverability.

ACKNOWLEDGEMENTS

The present work was supported by the YEQISUN Joint Funds of the National Science Foundation of China (Grant No. U2141228). The essential supports are greatly acknowledged.

REFERENCES

[1] Hoppe, K.G., Scale Effects in Manoeuvring Tests with Small Ship Model[J]. Maneuvering, 1972.

[2] Kajita, E., Mori, M., Yagi, T., Uosaki, S., et al., On the Manoeuverability of Ship have Small Length-beam Ratio (Scale Effect and Confirmation for Application) [C], Proceeding of the Society of Naval Architects of Japan 1975 Spring Conference, 1975, 137:166-176.

[3] Jin, Y., Duffy, J., Chai, S., et al. URANS Study of Scale Effects on Hydrodynamic Manoeuvring Coefficients of KVLCC2[J]. Ocean Engineering, 2016, 118:93-106.

[4] Liu, X., Nie, J., Xia, Z., & Fan, S., Investigation on the Scale Effect of Maneuverability Based on Model Tests and Sea Trials of a Ship[C]. International Society of Offshore and Polar Engineers, 2017.

[5] Duman, S. & Bal, S., Numerical Investigation of Scale Effects on Maneuvering Coefficients of DTMB 5415 hull[C]. 1st International Congress on Ship and Marine Technology, 2016.

[6] Araki, M., Scale Effects on Ship Maneuverability Using RANS[C]. ASME. International Conference on Offshore Mechanics and Arctic Engineering, 2018.

[7] Wang, X., Liu, L., Zhang, Z., Feng, D., Numerical Study of the Stern Flap Effect on Catamaran' Seakeeping Characteristic in Regular Head Waves[J]. Ocean Engineering, 2020, 206:107172.

[8] Feng, D., Yu, J., He, R., Zhang, Z., Wang, X., Free Running Computations of KCS with Different Propulsion Models[J]. Ocean Engineering, 2020, 214:107563.

[9] Feng, D., Ye, B., Zhang, Z., Wang, X., Numerical Simulation of the Ship Resistance of KCS in Different Water Depths for Model-Scale and Full-Scale[J]. Journal of Marine Science and Engineering, 2020, 8(10):745.

[10] Menter, F.R., Two-equation Eddy-viscosity Turbulence Models for Engineering Applications[J]. Aiaa Journal, 1994, 32:1598-1605.

[11] Xing, T., Stern, F., Factors of Safety for Richardson Extrapolation[J]. Journal of Fluids Engineering, Transactions of the ASME, 2010, 132:614031-640313.

[12] Carrica, P.M., Ismail, F., Hyman, M., et al., Turn and Zigzag Maneuvers of a Surface Combatant Using a URANS Approach with Dynamic Overset Grids[J]. Journal of Marine Science and Technology, 2013, 18(2).